Title

Sulcal morphology of posteromedial cortex substantially differs between humans and chimpanzees

Authors

Ethan H. Willbrand[1,2*], Samira A. Maboudian[2*], Joseph P. Kelly[1], Benjamin J. Parker[2], Brett L. Foster[3], Kevin S. Weiner[1,2]

[1]*Department of Psychology, University of California Berkeley, Berkeley, CA, 94720 USA*
[2]*Helen Wills Neuroscience Institute, University of California Berkeley, Berkeley, CA, 94720 USA*
[3]*Department of Neurosurgery, Perelman School of Medicine, University of Pennsylvania, Philadelphia, PA, 19104 USA*

*co-first authors

Corresponding authors: Kevin S. Weiner

Email: kweiner@berkeley.edu

Keywords: neuroanatomy, neuroimaging, comparative biology, cortical folding, posteromedial cortex

Conflict of Interest Statement: The authors declare no competing financial interests.

Acknowledgements: This research was supported by NSF CAREER Award 2042251 (Weiner) and NIH Grant R01MH129439 (Foster). Young adult neuroimaging and behavioral data were provided by the HCP, WU-Minn Consortium (Principal Investigators: David Van Essen and Kamil Ugurbil; NIH Grant 1U54-MH-091657) funded by the 16 NIH Institutes and Centers that support the NIH Blueprint for Neuroscience Research, and the McDonnell Center for Systems Neuroscience at Washington University. Chimpanzee data were provided by the National Chimpanzee Brain Resource (NIH Grant NS092988). We thank Willa Voorhies and Jacob Miller for their assistance developing the data collection pipeline used for this study, as well as Tyler Hallock, and Lyndsey Aponik Gremillion for their previous assistance defining posteromedial sulci in humans.

Author Contributions: E.H.W. and K.S.W. designed research. E.H.W., S.A.M., J.P.K., B.J.P., B.L.F., and K.S.W. performed research. E.H.W., S.A.M., and K.S.W. analyzed data. E.H.W., S.A.M., and K.S.W. wrote the paper. All authors edited the paper and gave final approval before submission.

Abstract

Recent studies identify a surprising coupling between evolutionarily new sulci and the functional organization of human posteromedial cortex (PMC). Yet, no study has compared this modern PMC sulcal patterning between humans and non-human hominoids. To fill this gap in knowledge, we first manually defined 918 sulci in 120 chimpanzee (*Pan Troglodytes*) hemispheres and 1619 sulci in 144 human hemispheres. We uncovered four new PMC sulci, and quantitatively identified species differences in incidence, depth, and surface area. Interestingly, some PMC sulci are more common in humans and others, in chimpanzees. Further, we found that the prominent marginal ramus of the cingulate sulcus differs significantly between species. Contrary to classic observations, the present results reveal that the surface anatomy of PMC substantially differs between humans and chimpanzees — findings which lay a foundation for better understanding the evolution of neuroanatomical-functional and neuroanatomical-behavioral relationships in this highly expanded region of the human cerebral cortex.

Introduction

A fundamental question in comparative biology and systems neuroscience is: What features of the brain are unique to humans? Key insights regarding what features of the brain are unique to humans have been gleaned from studies comparing anatomical and functional features of the human brain to features from the brains of our close evolutionary relative, the chimpanzee[1–20]. Of all the features to study, researchers particularly focus on the folds of the cerebral cortex, or sulci, as they generally track with evolutionary complexity[21]. For example, while mice and marmosets have rather smooth, lissencephalic cerebral cortices, 60-70% of the cerebral cortex in hominoids is buried within sulci[3,22]. Intriguingly, recent studies have identified "evolutionarily new" shallow sulci in association cortices in hominoid brains that have been linked to functional organization across a broad array of cognitive domains (e.g.,[14,19,23–38]), several of which reflect cognitive abilities that are arguably unique to humans. Building on this previous work, we compared the sulcal patterning of the posteromedial cortex (PMC) — a region on the medial cortical surface that includes the posterior cingulate, retrosplenial, and precuneal cortices[39] — between humans and chimpanzees with a particular emphasis on the smaller, shallower, and relatively overlooked "evolutionarily new" cortical indentations.

The sulcal organization of PMC has been under-documented, even in the most recent neuroanatomical treatises (e.g.,[40,41]). Nevertheless, PMC is critically important in hominoids as it contains regions implicated in the default mode and cognitive control networks[42–47] with complex structural and functional connections[39,44,47,48]. PMC is also implicated in many complex cognitive abilities[43,47,49–52] and is particularly susceptible to neurodegenerative disease[50]. Thus, quantifying the similarities and differences in the PMC sulcal patterning between chimpanzees and humans will not only shed light on the comparative neuroanatomy of PMC between species, but also

provide understanding regarding structural-functional relationships between species with potential cognitive insights[53].

While it is known that the larger (primary) sulci within PMC are present in chimpanzees[54–56] and the inframarginal sulcus — a newly uncovered smaller (tertiary) PMC sulcus — is variably present in chimpanzees[20], the phylogenetic emergence of a majority of recently clarified PMC sulci[20] has yet to be compared between chimpanzees and humans. Therefore, in the present study, we comprehensively examined the PMC sulcal patterning between humans and chimpanzees using cortical surface reconstructions as in our prior work[15,20,38]. Our analyses were guided by three main questions. First, does the amount of PMC buried in sulci differ between humans and chimpanzees? Second, do the incidence rates of PMC sulci differ between species? Third, do the primary morphological features of these structures (i.e., depth and surface area) differ between species?

Results

In order to answer these main questions, we examined the PMC of 72 young adult humans [from the Human Connectome Project (HCP; http://www.humanconnectomeproject.org/)] and 60 chimpanzees [from the National Chimpanzee Brain Resource (https://www.chimpanzeebrain.org/)]. These participants were used in prior work to assess the anatomical, functional, and evolutionary significance of a new tripartite landmark in PCC, the inframarginal sulcus (ifrms[20]), but the rest of the PMC sulci were not considered in these previous cross-species analyses until the present study.

To broadly determine how much of the PMC is sulcal vs. gyral in each species, we calculated how much of the regions corresponding to an automated parcellation of PMC in FreeSurfer[57] were buried in sulci (i.e., the percentage of vertices with values above zero in the .sulc

file[58]) via the Dice coefficient (**Fig. 1a**; **Materials and Methods**). Replicating prior postmortem work[3,22,59], the majority of human PMC was buried in sulci (mean ± std = 73.9 ± 1.97%). Chimpanzee PMC was relatively less sulcated (mean ± std = 67.4 ± 3.69%; **Fig. 1b**). A linear mixed effects model (LME) with factors of *species* and *hemisphere* (controlling for differences in brain size), confirmed this large difference between species (main effect of *species*: $F(1, 130) = 220.57$, $p < .0001$, $\eta 2 = 0.63$; no hemispheric differences: *p*s > .24; **Fig. 1b**).

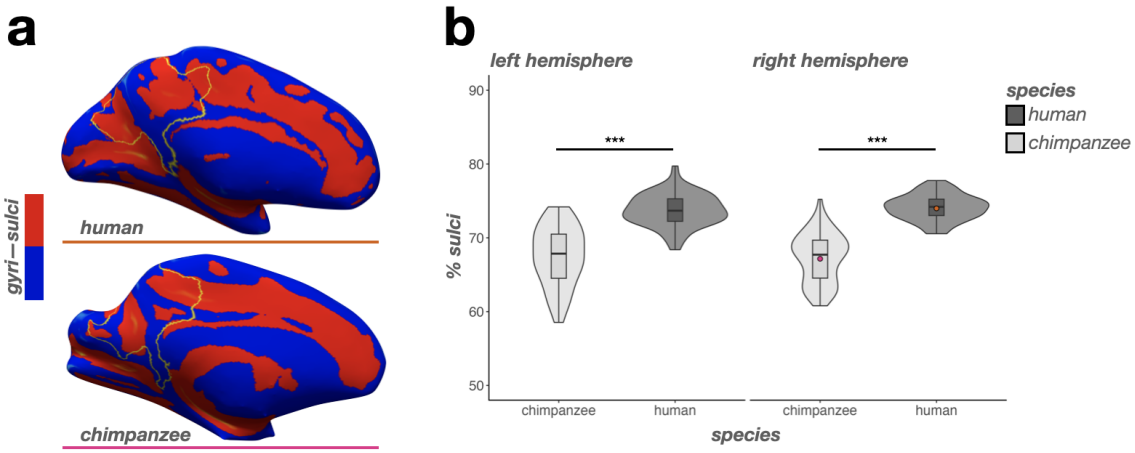

Figure 1. The percentage of PMC buried in sulci differs between humans and chimpanzees. a. Inflated human (top) and chimpanzee (bottom) right hemisphere cortical surface reconstructions (mirrored for visualization purposes). The outline of automatically defined PMC from the Destrieux parcellation[57] is indicated in yellow. The FreeSurfer .sulc file[58] is overlaid on each surface (Sulci: red; Gyri: blue). These surfaces present the average PMC sulcation for each species (Human: 73.9%; Chimpanzee: 67.4%). The lines below each surface correspond to the colored individual dots on the plot to the right. **b.** Violin plots (box plot and kernel density estimate) visualizing the percentage of PMC in sulci (percentage values are out of 100) as a function of species (x-axis) and hemisphere (left: left hemisphere; right: right hemisphere). The significant difference in PMC sulcation between species (as a result of the main effect of species) is indicated with asterisks (*** $p < .001$).

Next, we manually defined sulci in precuneal (PrC) and posterior cingulate cortices (PCC) — which are subregions of the PMC[20,39,47] — in all human and chimpanzee brains (**Materials and Methods** for a detailed description of these sulci). All PMC sulci were defined on cortical reconstructions from FreeSurfer (v6.0.0, surfer.nmr.mgh.harvard.edu; **Fig. 2** for example hemispheres; Supplementary Figs. 1-2 for all human and chimpanzee brains). Once all sulci were

defined, we quantified the average sulcal depth (normalized to the max depth in each hemisphere) and surface area (normalized to the total surface area of each hemisphere) of each PMC sulcus (**Materials and Methods**).

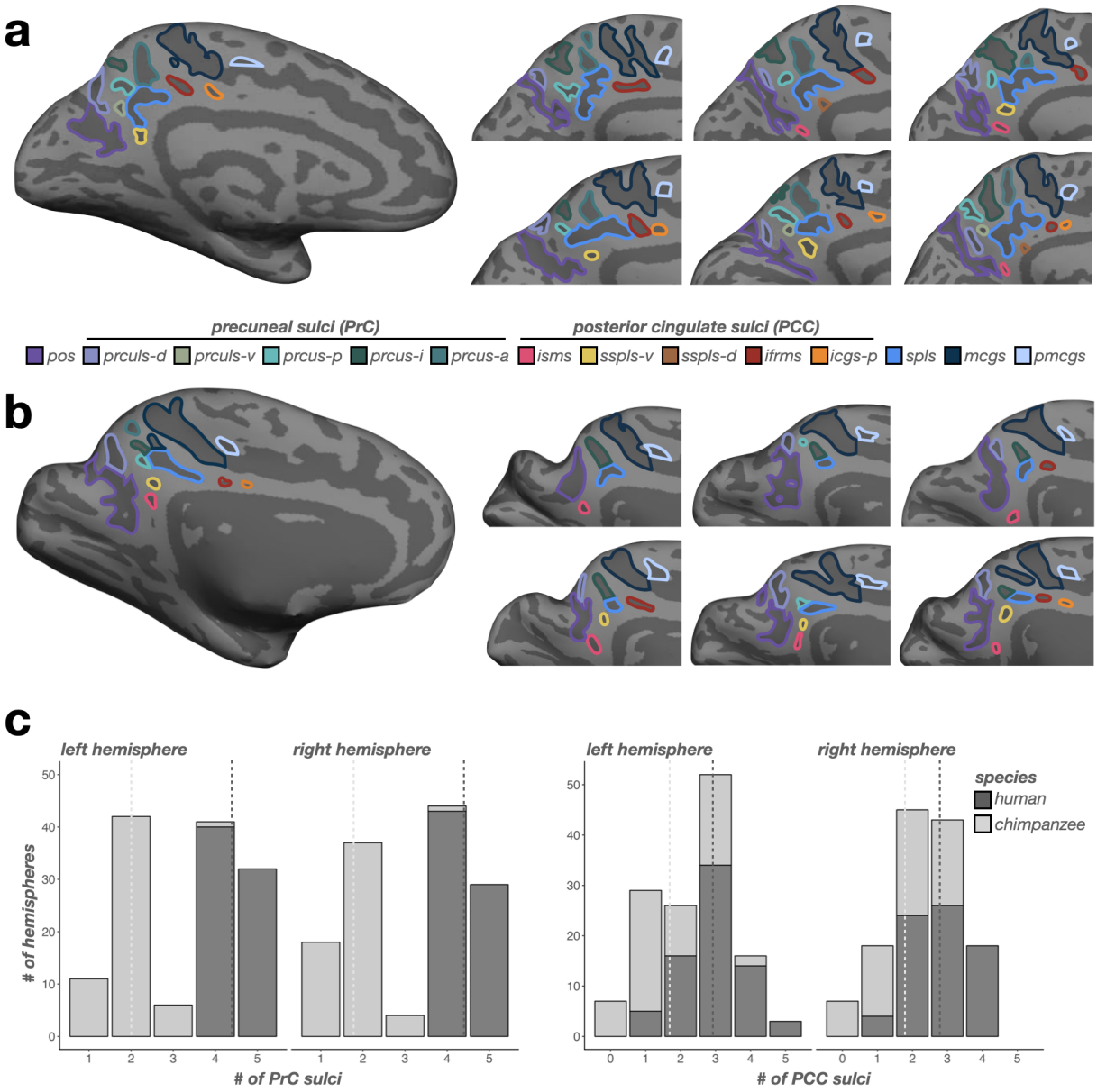

Figure 2. Humans have more PMC sulci than chimpanzees across hemispheres in both PrC and PCC. a. Left: An inflated cortical surface reconstruction of an individual human hemisphere. Sulci: dark gray; Gyri: light gray. Individual posteromedial (PMC) sulci are outlined according to the legend at the bottom. Right: Six example hemispheres zoomed in on the PMC depicting variations of sulcal incidence between participants. Right hemisphere images are mirrored so that all images have the same orientation. **b.** Same as a, but for chimpanzee hemispheres. **c.** Left: Incidence rates of precuneal (PrC) sulci (x-axis; see legend in a) across species (colors, see legend) for each

hemisphere (left: left hemisphere; right: right hemisphere). Dashed lines indicate the average number of sulci for each species in each hemisphere. Right: Same as the left, but for posterior cingulate (PCC) sulci.

Once sulci were defined, we quantified the incidence rates of PMC sulci in three groups: i) sulci that border, or serve as the bounding perimeter of, PMC, ii) PCC sulci, and iii) PrC sulci. Crucially, this procedure revealed four new PMC sulci that were not considered in prior work of PMC sulcal morphology (e.g.,[20,44,55,59–63]; **Fig. 2**, Supplementary Figs. 3-4). While we labeled and quantified the incidence rates of these four sulci across species for the first time, some present and modern anatomists often included an unlabeled sulcus in the location of some these sulci in their summary schematics (Supplementary Figs. 3-4). Further, these sulci were identifiable in postmortem chimpanzee hemispheres from a classic neuroanatomical atlas[56], ensuring that FreeSurfer's computational processes did not artificially create shallow sulci (Supplementary Fig. 4). We described across-species comparisons for each group in turn below using logistic regression GLMs with *species* (human, chimpanzee) and *hemisphere* (left, right), as well as their interaction, as factors for sulcal presence. Afterwards, we compared the depth and surface area of PMC sulci between species using LMEs with *species* (human, chimpanzee), *sulcus* (PMC sulci), and *hemisphere* (left, right), as well as their interaction, as factors. Finally, we repeat these analyses on the incidence and morphology of the marginal ramus of the cingulate sulcus — a prominent sulcal landmark in PMC[20,44,55,59–63] that contrary to previous studies, differs substantially between species, which we show here.

Incidence rates of large and deep sulci that border PMC do not differ across species, including the newly identified premarginal branch of the cingulate sulcus (pmcgs)

We identified the following three large and deep sulci serving as borders of PMC: the marginal ramus of the cingulate sulcus (mcgs), splenial sulcus (spls), and parieto-occipital sulcus (pos).

Replicating prior post-mortem work[54–56], we found that the mcgs, spls, and pos were present in all humans and chimpanzees (**Fig. 3**). We also identified a consistent sulcus just anterior to the mcgs (**Figs. 2-3**). As such, we refer to this sulcus as the premarginal branch of the cingulate sulcus (pmcgs). When present, the pmcgs is located just under the paracentral fossa and serves as the point where the mcgs breaks from the cingulate sulcus (cgs) proper (**Materials and Methods**). The pmcgs was clearly identifiable in 97.22% of left and 94.4% of right hemispheres in humans and in 100% of chimpanzees (**Fig. 3**). The incidence rates for these four sulci were comparable between species (no main effect of *species*: $\chi 2 = 2.45$, df = 1, $p = 0.12$; **Fig. 3**).

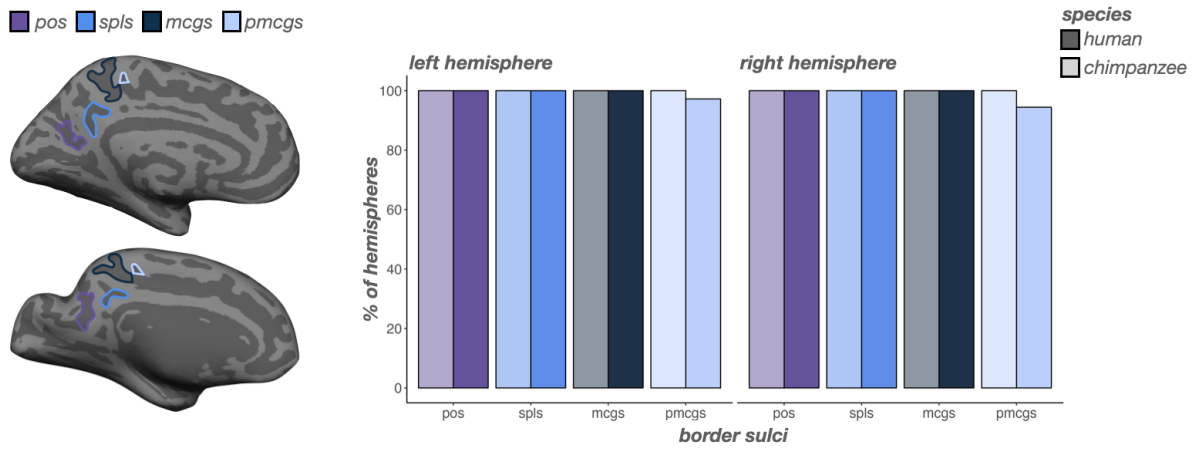

Figure 3. Incidence rates of sulci that border PMC are comparable between humans and chimpanzees. Left: An inflated cortical surface reconstruction of an individual human (top) and chimpanzee (bottom) hemisphere with sulci that border PMC outlined according to the legend at the top of the figure. Right: Bar plots visualizing incidence rates (percent of hemispheres) as a function of sulcus (x-axis), species (darker colors: human; lighter colors: chimpanzee), and hemisphere (left: left hemisphere; right: right hemisphere). Sulci are generally ordered posterior to anterior.

Incidence rates of PrC sulci differ substantially across species, including the newly identified ventral precuneal limiting sulcus (prculs-v)

In human PrC, the posterior (prcus-p), intermediate (prcus-i), and anterior precuneal sulci (prcus-a), as well as the dorsal precuneal limiting sulcus (prculs-d) were present in all hemispheres (**Fig. 4**). Previously, we[20] referred to this latter sulcus as the prculs (mirroring the label from a recent

183 neuroanatomical atlas[60]). However, here, we also consistently identified a ventral sulcal
184 component in a comparable posterior plane as the dorsal prculs, but more inferiorly situated
185 between the prculs-d and the spls (**Figs. 2, 4**). Consequently, we refer to this sulcus as the ventral
186 prculs (prculs-v), which was identifiable in 44.44% of left and 40.28% of right hemispheres in
187 humans (**Fig. 4**).

188 In contrast, PrC sulci were far more variable in chimpanzees. Generally, humans contained
189 more sulci than chimpanzees in PrC ($F(1, 130) = 1194.13$, $p < .0001$, $\eta 2 = 0.90$; no hemispheric
190 differences: *p*s > .14; **Fig. 2c**, left). The prculs-d was the only sulcus comparably present between
191 species (*left*: 96.67%; *right*: 96.67%; no main effect of *species*: $\chi 2 = 3.19$, df = 1, $p = 0.07$; **Fig. 4**).
192 Interestingly, among the three recently identified prcus components[20], prcus-i was the second most
193 present PrC sulcus in chimpanzees, but was still less present than in humans (*left*: 76.67%; *right*:
194 73.33%; main effect of *species*: $\chi 2 = 24.09$, df = 1, $p < .0001$; **Fig. 4**). Conversely, prcus-p (*left*:
195 15%; *right*: 5%; main effect of *species*: $\chi 2 = 125.39$, df = 1, $p < .0001$) and prcus-a (*left*: 6.67%;
196 *right*: 5%; main effect of *species*: $\chi 2 = 150.56$, df = 1, $p < .0001$) were quite rare in chimpanzees
197 (**Fig. 4**). Finally, the newly identified prculs-v in humans was not identifiable in any chimpanzee
198 hemispheres examined (main effect of *species*: $\chi 2 = 47.30$, df = 1, $p < .0001$; **Fig. 4**).

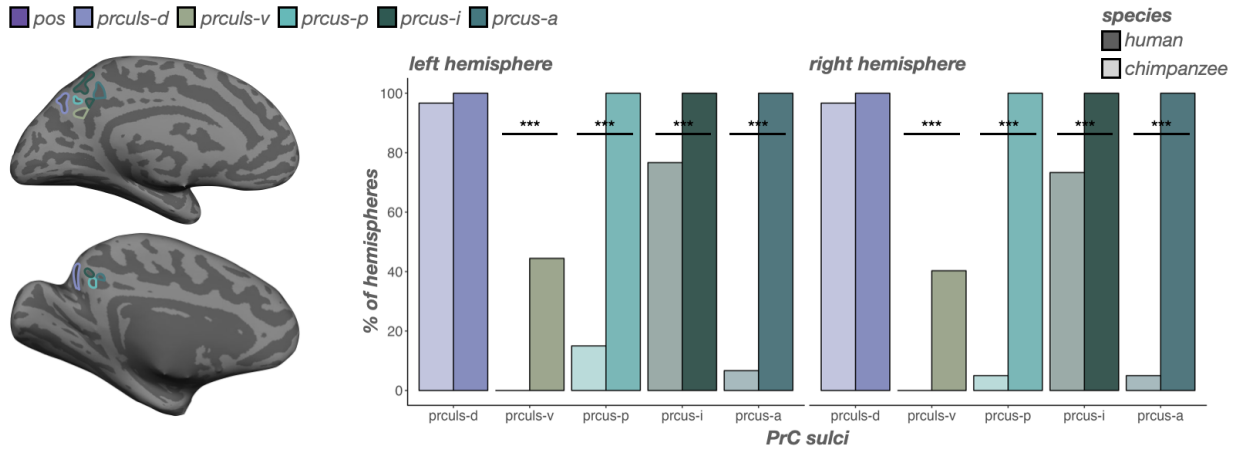

199

Figure 4. Incidence rates of precuneal (PrC) sulci are generally higher in humans than chimpanzees. Left: An inflated cortical surface reconstruction of an individual human (top) and chimpanzee (bottom) hemisphere with PrC sulci outlined according to the legend at the top of the figure. Right: Bar plots visualizing incidence rates (percent of hemispheres) as a function of sulcus (x-axis), species (darker colors: human; lighter colors: chimpanzee), and hemisphere (left: left hemisphere; right: right hemisphere). Sulci are generally ordered posterior to anterior. Lines and asterisks highlight significant differences in incidence between species (* $p < .05$, *** $p < .001$). The intermediate precuneal sulcus (prcus-i) is the most common of the three precuneal sulci in chimpanzees. In comparison to the consistency of the prcus-i, prcus-a and prcus-p are extremely rare in chimpanzees.

Incidence rates of PCC sulci differ substantially across species, in which the newly identified ventral subsplenial sulcus (sspls-v) and isthmus sulcus (isms) are identifiable as frequently or more frequently in chimpanzees than humans

Sulci in human PCC are more variable than those in human PrC (**Fig. 2**)[20]. Generally, humans contained more sulci in PCC ($F(1, 130) = 63.86$, $p < .0001$, $\eta 2 = 0.33$; no hemispheric differences: ps > .42; **Fig. 2c**, right) than chimpanzees. As shown previously, the inframarginal sulcus (ifrms) is the only PCC sulcus present in 100% of human hemispheres (**Fig. 5**)[20]. The ifrms is identifiable in 50% of chimpanzee hemispheres (**Fig. 5**)[20]. Anterior to the ifrms, the posterior intracingulate sulcus (icgs-p) was present in 65.28% of left and 66.67% right hemispheres in humans, and rarely identifiable in chimpanzees (*left*: 6.67%; *right*: 5%; main effect of *species*: $\chi 2 = 53.74$, $df = 1$, $p < .0001$; **Fig. 5**). Posterior to the ifrms, the dorsal subsplenial sulcus (sspls-d) was present in 47.22% of left and 50% right hemispheres in humans, and was not identifiable in any chimpanzee hemispheres (main effect of *species*: $\chi 2 = 51.02$, $df = 1$, $p < .0001$; **Fig. 5**).

While we previously referred to the sspls-d as the sspls[20], here, we also identified an additional sulcus that was consistently identifiable just ventral and discontinuous with the dorsal component (**Figs. 2, 5**). As such, we refer to this newly-identified sulcus as the ventral sspls (sspls-v), which in humans was present in 66.67% of left hemispheres and 48.61% of right hemispheres (**Fig. 5**). Interestingly, the sspls-v showed no main effect of *species* ($\chi 2 = 1.39$, $df = 1$, $p = 0.24$), but an interaction between *species* and *hemisphere* ($\chi 2 = 5.34$, $df = 1$, $p = 0.02$), such that in

chimpanzees it was present in a comparable amount of left hemispheres to humans (56.67%; p = 0.24, Tukey's adjustment), but was present in more chimpanzee right hemispheres than human right hemispheres (66.67%; odds ratio = 0.75, p = 0.03, Tukey's adjustment; **Fig. 5**).

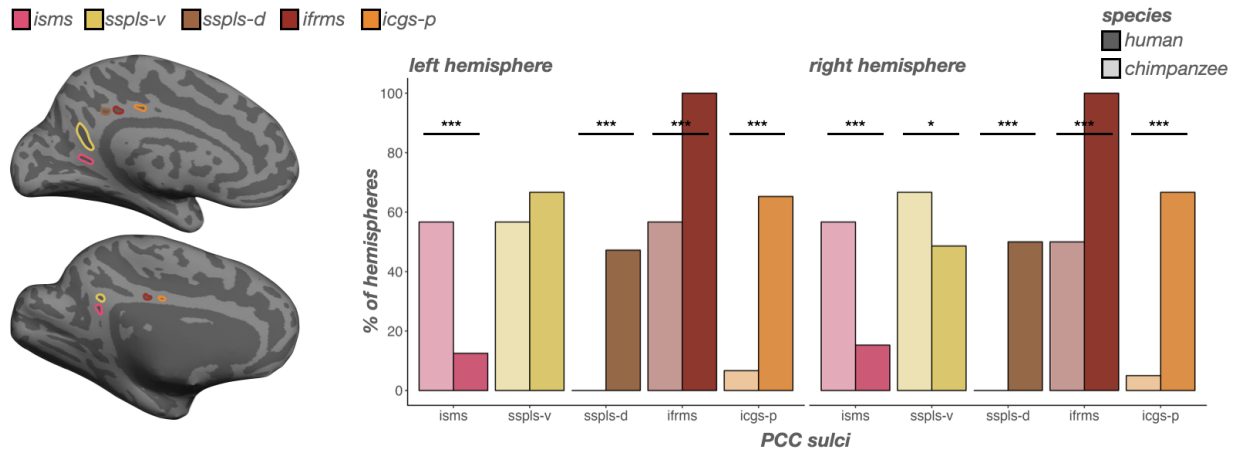

Figure 5. Incidence rates of posterior cingulate (PCC) sulci are variable between humans and chimpanzees. Left: An inflated cortical surface reconstruction of an individual human (top) and chimpanzee (bottom) hemisphere with PCC sulci outlined according to the legend at the top of the figure. Right: Bar plots visualizing incidence rates (percent of hemispheres) as a function of sulcus (x-axis), species (darker colors: human; lighter colors: chimpanzee), and hemisphere (left: left hemisphere; right: right hemisphere). Sulci are generally ordered posterior to anterior. Lines and asterisks highlight significant differences in incidence between species (* $p < .05$, *** $p < .001$). The isms and sspls-v are more common in chimpanzees than humans. The sspls-d, ifrms, and icgs-p are more common in humans than chimpanzees. ifrms data from[20].

Finally, in a minority of humans (12.50% of left and 15.28% of right hemispheres), we could identify a previously undefined sulcus inferior to the sspls-v within the isthmus of the cingulate gyrus, which we termed the isthmus sulcus (isms; **Figs. 2, 5**). The isms was present in more chimpanzee hemispheres (56.67% of left and right hemispheres) than humans (main effect of *species*: $\chi2 = 30.26$, df = 1, $p < .0001$; **Fig. 5**). Interestingly, the incidence of the two more common PCC sulci in chimpanzees (sspls-v and isms) were related in chimpanzees ($\chi2 = 7.01$, df = 1, $p = 0.008$), such that chimpanzees with an sspls-v were more likely to have an isms (odds ratio = 4.77; **Fig. 6**). No other sulcal incidence rates were related ($ps > .10$). To further summarize these relationships, there was a *PCC region* (dorsal PCC, ventral PCC) and *species* interaction on

sulcal presence ($\chi 2 = 74.79$, df = 1, $p < .0001$), such that, overall, dorsal PCC sulci (sspls-d, ifrms, and icgs-p) were less common in chimpanzees than humans (odds ratio = -2.33, $p < .0001$, Tukey's adjustment), whereas ventral PCC sulci (isms and sspls-v) were more common in chimpanzees than humans (odds ratio = 0.96, $p < .0001$, Tukey's adjustment; **Fig. 5**).

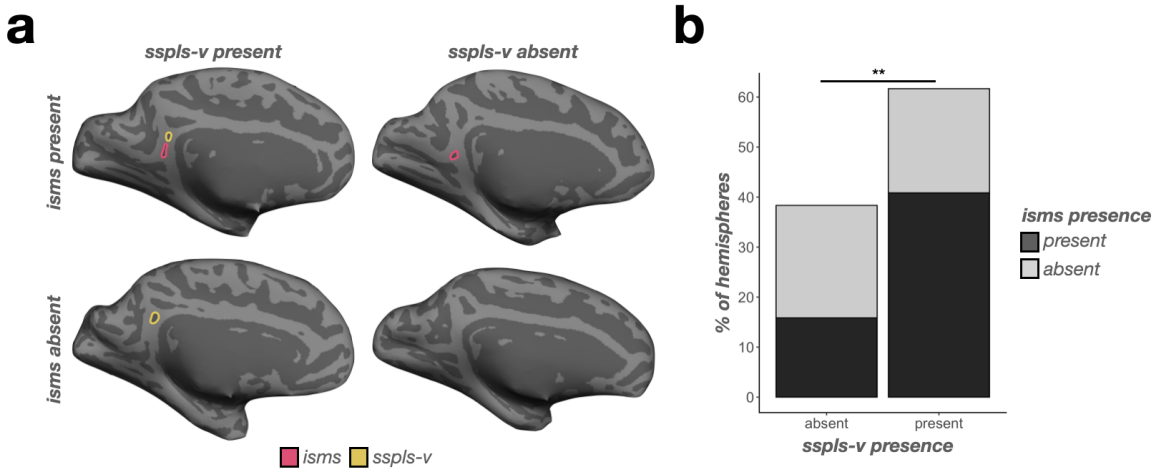

Figure 6. Incidence of the sspls-v is related to the incidence of the isms in chimpanzees. a. Four example inflated chimpanzee hemispheres displaying the four combinations of sspls-v (outlined in yellow when present) and isms (outlined in pink when present): both present (top left), sspls-v present (bottom left), isms present (top right), and both absent (bottom right). **b.** Bar plot visualizing the frequency of sspls-v and isms presence (colors, see legend). When the sspls-v is present, the isms is more likely present rather than absent; when the sspls-v is absent, the isms is likely to be absent (** $p < .01$).

The relative depth and surface area of PMC sulci largely differ between chimpanzees and humans

In terms of depth, a LME model with predictors of *sulcus*, *hemisphere*, and *species* revealed three *species*-related findings. First, a main effect of *species* ($F(1, 130) = 269.48$, $p < .0001$, $\eta 2 = 0.67$) showed that human PMC sulci were relatively deeper than chimpanzees (**Fig. 7a**). Second, an interaction between *species* and *sulcus* ($F(7, 1497) = 131.81$, $p < .0001$, $\eta 2 = 0.38$) indicated more complex relationships at the individual-sulcus level. Post hoc analyses revealed three findings: i) the isms, pos, prculs-d, prcus-i, spls, and sspls-v were relatively deeper in humans than chimpanzees (ps < .003, Tukey's adjustment), ii) the mcgs was relatively deeper in chimpanzees

than humans (p = .04, Tukey's adjustment), and iii) the pmcgs was comparably deep between species (p = .45, Tukey's adjustment; **Fig. 7a**). Third, a three-way interaction among *species*, *sulcus*, and *hemisphere* (F(7, 1497) = 2.43, p = .01, η2 = 0.01) showed that the mcgs was deeper in chimpanzees in the left hemisphere (p = .04, Tukey's adjustment), but comparably deep in the right hemisphere (p = .35, Tukey's adjustment; **Fig. 7a**) compared to humans.

In terms of surface area, a LME with predictors of *sulcus*, *hemisphere*, and *species* also revealed three *species*-related findings. First, a main effect of *species* (F(1, 130) = 6.51, p = .01, η2 = 0.05) showed that human PMC sulci were relatively larger than chimpanzees (**Fig. 7b**). Second, an interaction between *species* and *sulcus* (F(7, 1497) = 70.67, p < .0001, η2 = 0.25) indicated that the latter main effect was driven by differences at an individual-sulcus level. Post hoc analyses revealed three findings: i) the spls, prculs-d, and prcus-i were relatively larger in humans than chimpanzees (ps < .0001, Tukey's adjustment), ii) the pos, mcgs, and pmcgs were relatively larger in chimpanzees than humans (ps < .02, Tukey's adjustment), and iii) the isms and sspls-v were comparably large between species (ps > .62, Tukey's adjustment; **Fig. 7b**). Third, a three-way interaction among *species*, *sulcus*, and *hemisphere* (F(7, 1497) = 8.65, p < .0001, η2 = 0.04) showed that: i) the species difference for prculs-d was larger in the left hemisphere (estimate = -0.0015, p < .0001, Tukey's adjustment) than the right (estimate = -0.0008, p = .01, Tukey's adjustment), ii) the pmcgs was marginally relatively larger in chimpanzees in the left hemisphere (p = .05, Tukey's adjustment) but not the right hemisphere (p = .18, Tukey's adjustment), and iii) the pos is relatively larger in chimpanzees in the left hemisphere (p < .0001, Tukey's adjustment), but not the right hemisphere (p = .24, Tukey's adjustment; **Fig. 7b**).

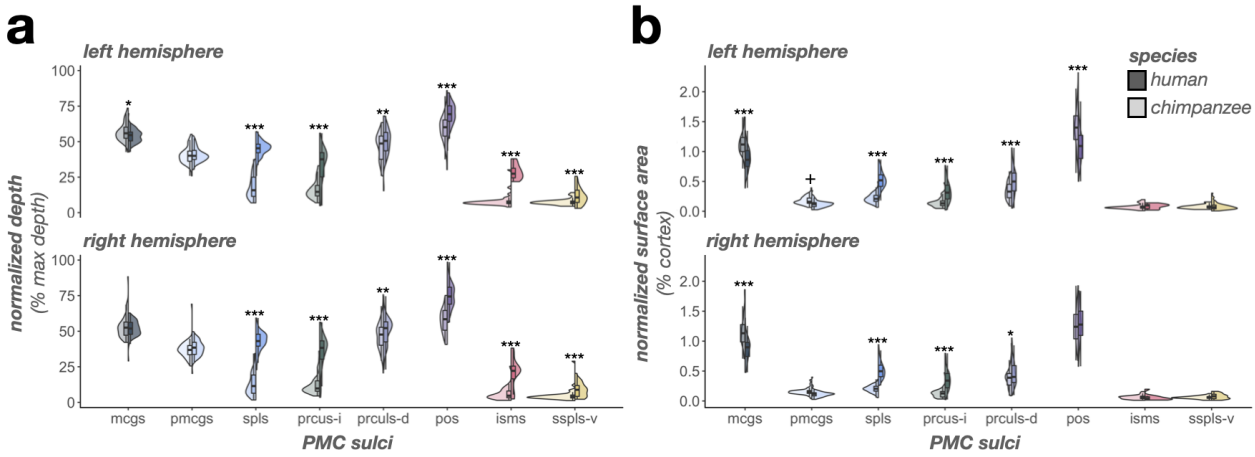

Figure 7. The complex relationship of PMC sulcal morphology in humans versus chimpanzees. a. Split violin plots (box plot and kernel density estimate) visualizing normalized sulcal depth (percent of max depth; percentage values are out of 100) as a function of sulcus (x-axis), species (darker colors, right violin: human; lighter colors, left violin: chimpanzee), and hemisphere (top: left hemisphere; bottom: right hemisphere). Significant differences between species [as a result of the species x sulcus interaction (or the species x sulcus x hemisphere interaction for the mcgs)] are indicated with asterisks (* $p < .05$, ** $p < .01$, *** $p < .001$). **b.** Same as a, but for normalized surface area (percent of cortical surface area; percentage values are out of 100). Significant differences between species [as a result of the species x sulcus interaction (or the species x sulcus x hemisphere interaction for the prculs-d, pmcgs, and pos)] are indicated with asterisks (+ $p = .05$; * $p < .05$, ** $p < .01$, *** $p < .001$).

Morphological types of the mcgs differ substantially between humans and chimpanzees

Previous work by Bailey and colleagues[55] showed that the chimpanzee mcgs bifurcated into what they termed "vertical" and "horizontal" components. Conversely, Ono and colleagues[61] identified that the human mcgs could variably present with side branches and/or a bifurcated dorsal end. In the present study, we integrated these previous classifications into four patterns based on what branches were present. We could identify up to three different branches of the mcgs: i) the main branch (mb) extending from the cingulate sulcus, ii) a branch extending dorsally from the main branch (db), and iii) a side branch (sb) extending horizontally or ventrally from the main branch (termed cih, as in Bailey *et al.*[55]). In the neuroanatomical literature, it is common to qualitatively describe sulcal "types" based on variation in the shape of a given sulcus and/or patterning of fractionation or intersection with neighboring sulci (e.g.,[32,64–66]). Following this terminology, the

combination of these branches fell into four types: I) an mb with no db or sb, II) mb with a db, III) mb with a sb, and IV) mb with both a db and sb (**Fig. 8a**).

We quantitatively determined whether the incidence rates of the four mcgs types differed by species, as well as between hemispheres for each species with chi-squared ($\chi 2$) tests. We observed significant differences in both hemispheres (*left*: $\chi 2 = 61.95$, df = 3, $p < .0001$; *right*: $\chi 2 = 52.62$, df = 3, $p < .0001$; **Fig. 8b**). Specifically, type I was comparably present between species in both the left ($p = .24$; *chimpanzee*: 3.33%; *human*: 9.72%) and right hemispheres ($p = .34$; *chimpanzee*: 3.33%; *human*: 6.94%; **Fig. 8b**). Type II was more present in chimpanzees (and the most common type) than humans in both the left ($p < .0001$; *chimpanzee*: 68.33%; *human*: 8.33%) and right hemispheres ($p < .0001$; *chimpanzee*: 53.33%; *human*: 6.94%; **Fig. 8b**). Conversely, type III was only present in humans (and the most common type) in both the left ($p < .0001$; *chimpanzee*: 0%; *human*: 43.06%) and right hemispheres ($p < .0001$; *chimpanzee*: 0%; *human*: 44.44%; **Fig. 8b**). Finally, type IV was equally present in both the left ($p = .13$; *chimpanzee*: 28.33%; *human*: 38.89%) and right hemispheres ($p = .69$; *chimpanzee*: 43.33%; *human*: 41.67%; **Fig. 8b**) across species. There was no hemispheric asymmetry in either species (*chimpanzee*: $\chi 2 = 2.99$, df = 2, $p = .22$; *human*: $\chi 2 = 0.51$, df = 3, $p = .92$; **Fig. 8b**).

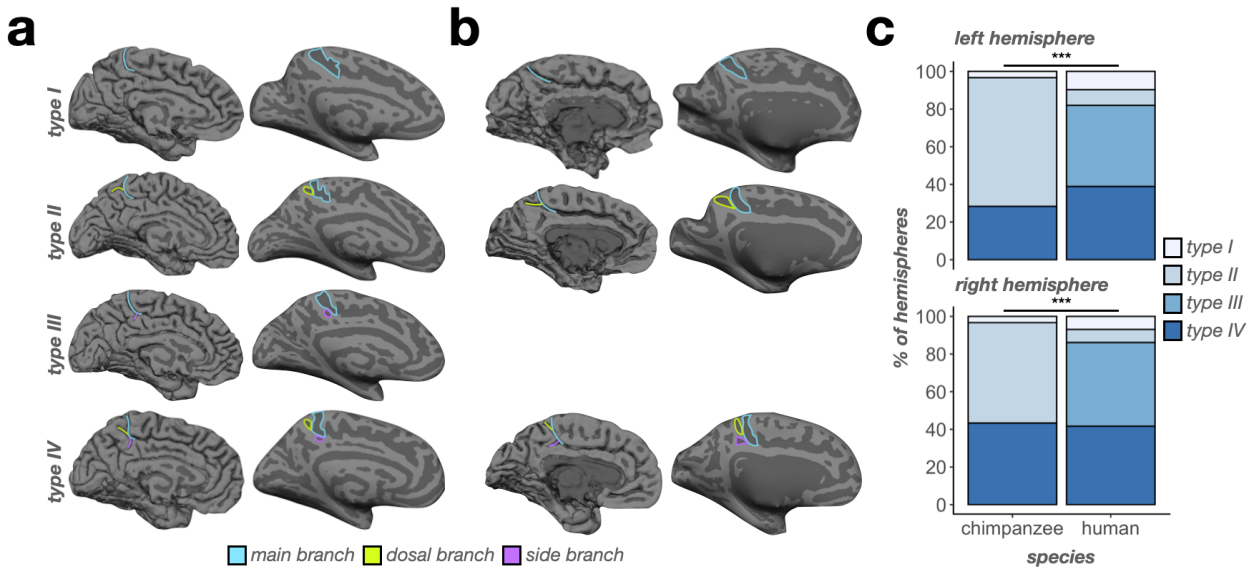

Figure 8. Chimpanzees do not have a Type III mcgs. a. Example pial (left) and inflated (right) human hemispheres displaying the four "types" of the mcgs. Type I consists of only a main branch (blue outlines/lines). Type II consists of a main branch and a dorsal branch (green outlines/lines). Type III consists of a main branch and a side branch (purple outlines/lines). Type IV consists of all three branches. **b.** Same as a, but for chimpanzees. Note that no chimpanzees in our sample had an identifiable type III mcgs (empty third row). **c.** Bar plot visualizing the incidence of mcgs types as a function of species (x-axis), type (color, see legend), and hemisphere (top: left hemisphere; bottom: right hemisphere). Lines and asterisks highlight significant species differences in the incidence of mcgs types in both hemispheres (*** $p < .001$).

The depth and surface area of mcgs components largely differ between chimpanzees and humans

Finally, we quantitatively tested for species differences in the sulcal depth and surface area of the three mcgs components comprising the different types (mb, db, and sb). In terms of depth, a LME with predictors of *component*, *hemisphere*, and *species* on mcgs component sulcal depth revealed five findings. First, there was a main effect of *component* ($F(2, 341) = 440.90$, $p < .0001$, $\eta 2 = 0.72$), such that the mb was deeper than the db and sb ($ps < .0001$, Tukey's adjustment) and the db was deeper than the sb ($p < .0001$, Tukey's adjustment; **Fig. 9a**). Second, there was a main effect of *hemisphere* ($F(1, 130) = 25.25$, $p < .0001$, $\eta 2 = 0.16$), such that components of the mcgs are generally deeper in the left than right hemisphere (**Fig. 9a**). Third, there was a main effect of *species* ($F(1, 130) = 17.29$, $p < .0001$, $\eta 2 = 0.12$) in which chimpanzee mcgs components were

relatively deeper than humans (**Fig. 9a**). Fourth, there was an interaction between *species* and *component* ($F(2, 341) = 12.76$, $p < .0001$, $\eta 2 = 0.07$). Post hoc analyses revealed that the db ($p < .0001$, Tukey's adjustment) and mb ($p = .03$, Tukey's adjustment) of the mcgs were relatively deeper in chimpanzees, whereas the sb was comparably deep between species ($p = .99$, Tukey's adjustment; **Fig. 9a**). Fifth, there was a three-way interaction among *species*, *component*, and *hemisphere* ($F(2, 341) = 5.58$, $p = .004$, $\eta 2 = 0.03$). Post hoc analyses revealed that it was driven by i) the mb of the mcgs being relatively deeper in chimpanzees in the left hemisphere ($p = .03$, Tukey's adjustment), but not the right ($p = .32$, Tukey's adjustment; **Fig. 9a**) and ii) the species difference (i.e., chimpanzee > human) for the db being larger in the right hemisphere (estimate = 0.11, $p < .0001$, Tukey's adjustment) than the left (estimate = 0.04, $p = .02$, Tukey's adjustment).

In terms of surface area, a LME with *component*, *hemisphere*, and *species* on mcgs component as predictors revealed two findings. First, there was a main effect of *component* ($F(2, 341) = 971.27$, $p < .0001$, $\eta 2 = 0.85$), such that the mb was larger than the db and sb ($ps < .0001$, Tukey's adjustment) and the db was larger than the sb ($p < .0001$, Tukey's adjustment; **Fig. 9b**). Second, there was a main effect of *species* ($F(1, 130) = 39.67$, $p < .0001$, $\eta 2 = 0.23$) in which the mcgs components were all relatively larger in chimpanzees compared to humans (**Fig. 9b**). There were no *species*-related interactions ($ps > .16$).

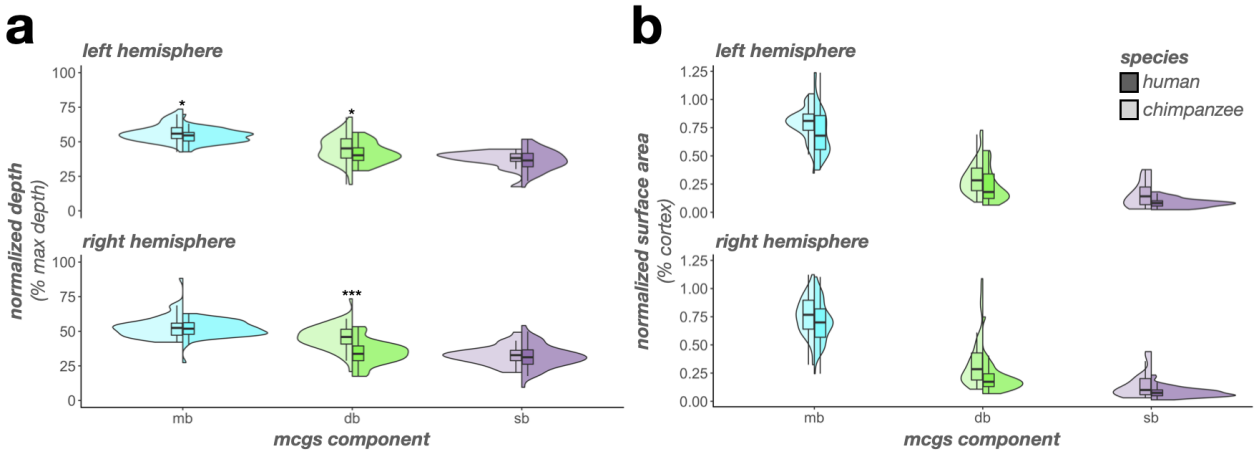

Figure 9. The mcgs is morphologically distinct between humans and chimpanzees. a. Split violin plots (box plot and kernel density estimate) visualizing normalized sulcal depth (percent of max depth; percentage values are out of 100) as a function of mcgs component (x-axis), species (darker colors, right violin: human; lighter colors, left violin: chimpanzee), and hemisphere (top: left hemisphere; bottom: right hemisphere). Significant differences between species (as a result of the species x component x hemisphere interaction) are indicated with asterisks (* $p < .05$, *** $p < .001$). **b.** Same as a, but for normalized surface area (percent of cortical surface area; percentage values are out of 100). Note that there was a main effect of species ($p < .0001$), such that mcgs components were relatively larger in chimpanzees than in humans. There were no interactions with component. db: dorsal branch; mb: marginal branch; sb: side branch

Discussion

By manually defining 2,537 sulci spanning the PMC of 144 human and 120 chimpanzee (*Pan Troglodytes*) hemispheres, we show that the surface anatomy of PMC substantially differs between these two hominoid species along three sulcal metrics: i) incidence/patterning, ii) depth, and iii) surface area (**Fig. 10** summarizes the major differences in PMC sulcal morphology between chimpanzees and humans). For sulcal incidence rates, half of PMC sulci are less present in chimpanzees than humans, whereas the other half are either more present in chimpanzees or equally present between species (**Fig. 10**). Further, the prominent mcgs differs significantly between species (**Fig. 10**). For sulcal depth, the majority of PMC sulci are relatively shallower in chimpanzees compared to humans; however, a minority are relatively deeper in chimpanzees or equally deep in both species (**Fig. 10**). For sulcal surface area, the majority of PMC sulci are relatively smaller in chimpanzees compared to humans; however, a minority are relatively larger in chimpanzees or equally sized across species (**Fig. 10**). This variability is in stark contrast to previous work claiming similarities between PMC between species:

"Overall, the medial aspect of the parietal lobe of the chimpanzee and other apes closely resembles the general appearance of the same structures in the human brain (Bailey et al., 1950)" [Cavanna and Trimble[67], pg. 565]

In the following sections, we discuss these findings in the context of the evolution of the cerebral cortex and the evolution of complex brain functions and behaviors, as well as discuss limitations and implications for future studies.

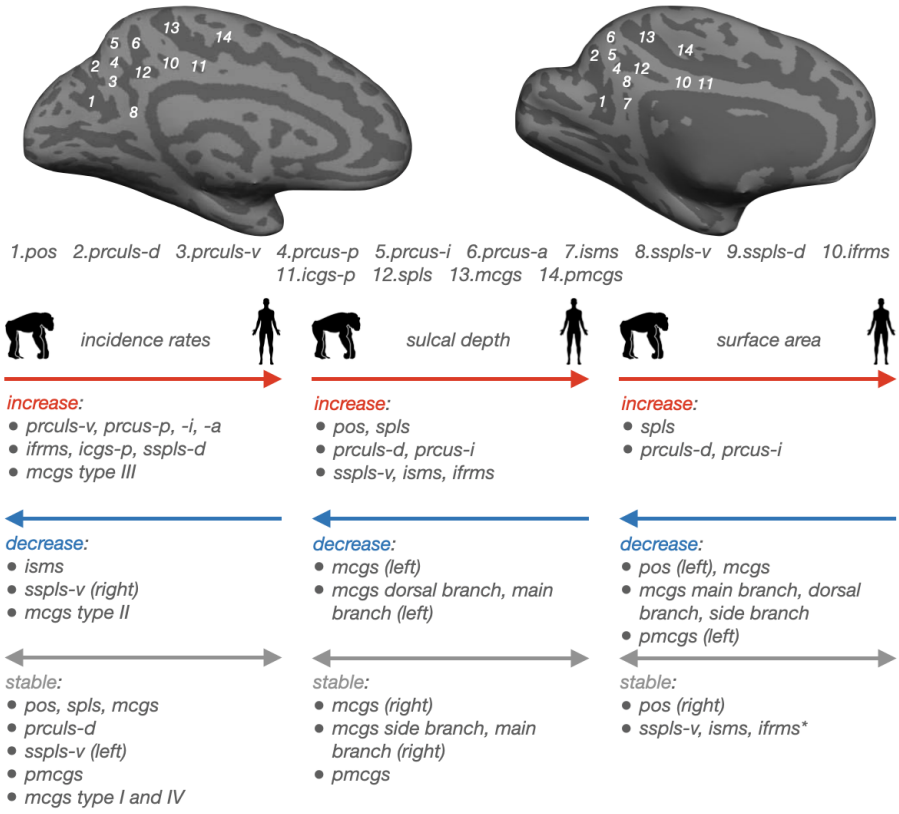

Figure 10. Summary of differences in PMC sulcal morphology between humans and chimpanzees. Top: Inflated cortical surface reconstructions of the individual human (Left) and chimpanzee (Right) hemispheres shown in Figure 2. Sulci: dark gray; Gyri: light gray. Individual posteromedial (PMC) sulci are numbered according to the key below. Bottom: Overview of differences in PMC sulcal morphology between species. Position (right, left, both) of arrowheads indicates whether sulci increased (right), decreased (left), or remained stable (right and left) in each morphological feature between species. *Left:* incidence rates; *Middle:* sulcal depth; *Right:* surface area. ifrms data from[20].

The present work adds to the growing literature in comparative neurobiology and paleoneurobiology classifying the presence/absence of sulci across species as a qualitative and quantitative metric to assess the evolution of the cerebral cortex. Such studies have revealed that although the sulcal patterning of primary sensory cortices more or less resembles one another

411 across species, this relationship is far less consistent in association cortices. For example, while
412 the sulcal organization of visual association cortex was comparable between every human and
413 non-human hominoid hemisphere examined in previous work[15], the incidence of sulci in
414 medial[14,16,17] and lateral[38] prefrontal cortex, as well as orbitofrontal cortex[64] was substantially
415 different across species. Adding to the complexity, within each of these regions, differences in
416 sulcal incidence rates were greater for some sulci compared to others — elucidating specific areas
417 of cortex that are particularly expanded/more complex in humans. For example, sulcal incidence
418 between humans and chimpanzees in the lateral prefrontal cortex is more consistent across species
419 in the posterior middle frontal gyrus than anterior middle frontal gyrus[38]. Further, some sulci in
420 the human prefrontal cortex are not present in non-human hominoids[2,19]. As shown in the present
421 study, although the PMC (at a regional level) is generally more evolutionarily expanded in
422 humans[68], the differences in PMC sulcal morphology between humans and chimpanzees was
423 heterogeneous—that is, not all sulci were less present, relatively smaller, and relatively shallower
424 in chimpanzees compared to humans (**Fig. 10**).

425 Here, we consider two different underlying features that could contribute to this observed
426 heterogeneity: i) differences in the size and depth of border sulci that constrain the
427 macroanatomical definition of PrC and PCC in each species and ii) expansion of PrC, but not PCC,
428 sulci between humans and chimpanzees. First, the main border sulci (pos and mcgs) were relatively
429 smaller and shallower in humans compared to chimpanzees (**Fig. 10**). This finding could be a
430 consequence of the large increase in size, depth, and number of PrC sulci observed in humans
431 compared to chimpanzees (**Fig. 10**). This observation is consistent with the classic compensation
432 theory of cortical folding by Connolly[69,70], which qualitatively states that the depth and size of
433 sulci are seemingly counterbalanced by those of their neighbors. In terms of the compensation

theory then, in chimpanzees, the shallow, small (or even absent) precuneal sulci neighbor large and deep pos and mcgs (and the reverse in humans), such that the former "compensate" for the latter and in turn, make the overall degree of cortical folding approximately equal[71]. Second, PrC sulci were relatively larger in humans compared to chimpanzees, whereas PCC sulci were not (**Fig. 10**). This could be a consequence of the PrC not being topographically constrained along the vertical axis, in contrast to the PCC which is constrained superiorly by the cingulate/splenial sulci and inferiorly by the callosal sulcus. Recent empirical evidence[10] supports this notion, finding that the PrC is the only area of PMC that spatially expands (in the longitudinal direction) between chimpanzees and humans. The majority of sulci in PrC and PCC were also relatively deeper in humans than chimpanzees, which could be due to the fact that both areas are not topographically constrained along this axis. Finally, the decrease in isms presence in humans (**Fig. 10**) may be a consequence of changes in pos morphology in humans. In nearly all human hemispheres, the pos intersects with the calcarine sulcus (e.g.,[61,72–75]), which is not necessarily the case in chimpanzees[54–56,72,76,77]. The intersection of these two sulci, which is in the proximity of the isms, may have led to its absence in humans. Considering that the present work only examined the PMC in chimpanzees, future work should seek to also examine the sulcal morphology of PMC in additional species such as macaques, baboons, bonobos, gorillas, orangutans, and gibbons in order to build a larger picture for how the PMC changes along the primate phylogeny.

The present findings also lay the foundation to examine the cognitive and functional role of PMC sulci in species beyond humans. Recent work shows that sulcal morphology relates to the appearance of complex behaviors in non-human hominoids[19,35,78,79]. For example, asymmetries in the depth of multiple sulci[19,35,78], as well as the presence of the paracingulate sulcus[35] and dorsal fronto-orbital sulcus pattern[19], relates to the production and use of attention-getting sounds by

chimpanzees. Further, asymmetries in the depth of the inferior arcuate sulcus was related to gestural communication in baboons[79], as was the presence of the intralimbic sulcus in chimpanzees[35]. Thus, a goal for future work would be to relate the incidence rates and morphological features of PMC sulci to behavioral performance in non-human hominoids.

In conclusion, our findings provide insight regarding how PMC sulcal patterning and morphology differs between humans and our close relative: the chimpanzee. We not only uncover the presence of previously overlooked structures in human and chimpanzee PMC, but also show that the sulcal organization of PMC differs dramatically between chimpanzees and humans along multiple metrics: percent sulci, sulcal presence, surface area, and depth. Future research can seek to further explore how the PMC sulcal patterning differs in humans relative to other non-human hominoids and non-human primates, as well as link the morphology of these structures to the emergence of complex behaviors and functional areas.

Materials and Methods

Participants:

Humans: Data for the young adult human cohort analyzed in the present study were taken from the Human Connectome Project (HCP) database (https://www.humanconnectome.org/study/hcp-young-adult/overview). Here we used data from 72 randomly selected participants (36 females, 36 males, aged between 22 and 36). HCP consortium data were previously acquired using protocols approved by the Washington University Institutional Review Board. Here, we used the same participants used in our previous work in PMC identifying the ifrms for the first time[20].

Chimpanzees: 60 (37 female, 23 male, aged between 9 and 51) chimpanzee (*Pan Troglodytes*)

anatomical T1 scans were chosen from the National Chimpanzee Brain Resource (www.chimpanzee brain.org; supported by NIH grant NS092988). The chimpanzees were members of the colony housed at the Yerkes National Primate Research Center (YNPRC) of Emory University. All methods were carried out in accordance with YNPRC and Emory University's Institutional Animal Care and Use Committee (IACUC) guidelines. Institutional approval was obtained prior to the onset of data collection. Further data collection details are described in Keller *et al*.[5]. Here, we examined the same chimpanzees used in our prior work in PMC and other cortical expanses[20,15,38].

Data Acquisition

Humans: Anatomical T1-weighted (T1-w) MRI scans (0.8 mm voxel resolution) were obtained in native space from the HCP database. First, the images obtained from the scans were averaged. Then, reconstructions of the cortical surfaces of each participant were generated using FreeSurfer, a software used for processing and analyzing human brain MRI images (v6.0.0, surfer.nmr.mgh.harvard.edu). All subsequent sulcal labeling and extraction of anatomical metrics were calculated from the cortical surface reconstructions of individual participants generated through the HCP's custom-modified version of the FreeSurfer pipeline[80].

Chimpanzees: Detailed descriptions of the scanning parameters have been described in Keller *et al.*[5], but we also describe the methods briefly here. Specifically, T1-weighted magnetization prepared rapid-acquisition gradient echo (MPRAGE) MR images were obtained using a Siemens 3T Trio MR system (TR = 2300 ms, TE = 4.4 ms, TI = 1100 ms, flip angle = 8, FOV = 200 mm) at YNPRC in Atlanta, Georgia. Before reconstructing the cortical surface, the T1 of each

chimpanzee was scaled to the size of the human brain. As described in Hopkins *et al.*[81], within FSL, the BET function was used to automatically strip away the skull, (2) the FAST function was used to correct for intensity variations due to magnetic susceptibility artifacts and radio frequency field inhomogeneities (i.e., bias field correction), and (3) the FLIRT function was used to normalize the isolated brain to the MNI152 template brain using a 7 degree of freedom transformation (i.e., three translations, three rotations, and one uniform scaling), preserved the shape of individual brains. Next, each T1 was segmented using FreeSurfer. The fact that the brains are already isolated, both bias-field correction and size-normalization, greatly assisted in segmenting the chimpanzee brain in FreeSurfer. Furthermore, the initial use of FSL also has the specific benefit, as mentioned above, of enabling the individual brains to be spatially normalized with preserved brain shape, and the values of this transformation matrix and the scaling factor were saved for later use.

Manual sulcal labeling: all PMC sulci

Humans: For the present study, we re-assessed the 144 human hemispheres analyzed in our prior work[20]. Manual lines were drawn on the FreeSurfer *inflated* cortical surface to define sulci with tools in *tksurfer* based on the most recent schematics of sulcal patterning in PMC by Petrides[60], as well as by the pial and smoothwm surfaces of each individual as in our prior work[20,27,28,36]. In some cases, the precise start or end point of a sulcus can be difficult to determine on a surface[82]. Thus, using the inflated, pial, and smoothwm surfaces of each individual to inform our labeling allowed us to form a consensus across surfaces and clearly determine each sulcal boundary. For each hemisphere, the location of PMC sulci was identified by trained raters (E.H.W., S.A.M., J.K., B.P., T.H., L.A.G.) and confirmed by a trained neuroanatomist (K.S.W.).

In this process, we started with the large and deep sulci that bound PMC. Specifically, PMC is bounded posteriorly and anteriorly by the parieto-occipital sulcus (pos) and marginal ramus of the cingulate sulcus (mcgs), respectively. The splenial sulcus (spls) serves as a boundary between two subregions of PMC, the (superior) precuneus (PrC) and (inferior) posterior cingulate cortex (PCC), from one another[20,59]. In the present study, we could also identify a previously unidentified sulcal component of the cingulate sulcus residing between the mcgs and paracentral sulcus[14,60] and below the paracentral fossa[60], which we term the premarginal branch of the cingulate sulcus (pmcgs). Broadly, this sulcus marks the point at which the mcgs extends from the main body of the cingulate sulcus.

As shown in previous work[20], there are four consistent sulci within PrC: the dorsal precuneal limiting sulcus (prculs-d) and three precuneal sulci (posterior: prcus-p, intermediate: prcus-i, anterior: prcus-a). Within PCC, our prior work identified three small and shallow sulci[20]. The inframarginal sulcus (ifrms) is present in every human hemisphere inferior to the mcgs. Anterior to the ifrms, there is a variably present indentation termed the posterior intracingulate sulcus (icgs-p) based on the intracingulate sulcus nomenclature by Borne and colleagues[82]. Posterior to the ifrms is the dorsal subsplenial sulcus (sspls-d) which is directly inferior to the main body of the spls.

In the present study, we identified three additional sulci not previously considered. The first sulcus is directly inferior to the posterior portion of the spls and more ventral along PCC —the ventral subsplenial sulcus (sspls-v) that is positioned underneath the sspls-d (when present). The second sulcus is posterior to prcus-p and inferior to the prculs-d—the ventral precuneal limiting sulcus

549 (prculs-v). The third is a previously uncharted and lone indentation appearing within the isthmus
550 of the cingulate gyrus, which we accordingly term the isthmus sulcus (isms). See **Fig. 2A** for 7
551 example human hemispheres with PMC sulci defined, and Supplementary Fig. 1 for every
552 hemisphere with sulcal labels.
553
554 *Chimpanzees:* Guided by recent in vivo criteria for defining PMC sulci in humans[20], we defined
555 PMC sulci in chimpanzees. Prior work leveraging this same chimpanzee sample determined that
556 chimpanzees variably possess an ifrms[20] and it is known that chimpanzees possess an mcgs, pos,
557 and spls[54–56]. Therefore, in the present study, we determined whether or not chimpanzees possessed
558 the pmcgs, as well as the five PrC sulci (prculs-d, prculs-v, prcus-p, prcus-i, prcus-a) and the four
559 other PCC sulci (isms, sspls-v, sspls-d, icgs-p) residing within the bounds of the mcgs, pos, and
560 spls in humans. As with humans, PMC sulci were defined in FreeSurfer using *tksurfer* tools, and
561 for each hemisphere, the location of PMC sulci was confirmed by the same two-tiered process.
562 See **Fig. 2B** for 7 example chimpanzee hemispheres with PMC sulci defined, and Supplementary
563 Fig. 2 for every hemisphere with sulcal labels.
564
565 <u>Manual sulcal labeling: mcgs patterns</u>
566 Linking to prior work by Bailey and colleagues[55] and Ono and colleagues[61], all 144 human and
567 120 chimpanzee inflated hemispheres were inspected by authors E.H.W., S.A.M., and K.S.W. to
568 determine which of the four mcgs patterns was present in humans and chimpanzees: I) a main
569 branch (mb) with no dorsal branch (db) or side branch (sb), II) mb with a db, III) mb with a sb,
570 and IV) mb with both a db and sb.
571

572 Calculating the amount of cortex buried in PMC across species

573 To quantify the amount of cortex buried in PMC across individuals and species, we combined six
574 regions in the Destrieux parcellation[57] corresponding to PMC: *G_cingul-Post-dorsal, G_cingul-*
575 *Post-ventral, G_precuneus, S_cingul-Marginalis, S_parieto_occipital, and S_subparietal*
576 (https://surfer.nmr.mgh.harvard.edu/fswiki/CorticalParcellation). These labels were converted
577 from the Destrieux annotation into individual labels and combined into one "PMC ROI"
578 FreeSurfer label with the *mri_annot2label* and *mri_mergelabels* functions in FreeSurfer. To
579 quantify the areas of the cortex defined as sulci, we used the .sulc file[58]. Depth values in the .sulc
580 file are calculated based on how far removed a vertex is from what is referred to as a "mid-surface,"
581 which is determined computationally so that the mean of the displacements around this "mid-
582 surface" is zero. Thus, generally, gyri have negative values, while sulci have positive values. To
583 create a "sulci ROI" FreeSurfer label, we thresholded the .sulc file for all vertices with values > 0
584 with the *mri_binarize* function in FreeSurfer. To determine the percent of PMC composed of sulci,
585 we calculated the overlap between the PMC ROI and sulci ROI with the Dice coefficient[20,36]:

586 $$DICE\ (X,Y)\ =\ \frac{2\,|X\ \cap\ Y|}{|X|\ +\ |Y|}$$

587 where X and Y are the PMC ROI and sulci ROI, $|\ \ |$ represents the number of elements in a set,
588 and ∩ represents the intersection of two sets.

589 We then ran a linear mixed effects model (LME) with predictors of hemisphere and species,
590 as well as their interaction terms, for percent overlap. Species and hemisphere were considered
591 fixed effects. Hemisphere was nested within subjects. We controlled for differences in brain size
592 in the model (quantified as the total cortical surface area of the given hemisphere). Analysis of
593 variance (ANOVA) F-tests were subsequently applied.

594

595 Analyzing differences in sulcal incidence:

596 *PMC sulci:* We characterized the frequency of occurrence of each sulcus separately for left and
597 right hemispheres. In line with prior work[14], for any sulcus that was not present in all hemispheres
598 for either species, we tested the influence of species and hemisphere on the probability of a sulcus
599 to be present with binomial logistic regression GLMs. For each statistical model, species (human,
600 chimpanzee) and hemisphere (left, right), as well as their interaction, were included as factors for
601 presence [0 (absent), 1 (present)] of a sulcus.

602 To compare whether the incidence of the variable PMC sulci in chimpanzees related to one
603 another, we ran binomial logistic regression GLMs for each variable PMC sulcus [0 (absent), 1
604 (present)] with the other sulci as factors, while also including an interaction with hemisphere for
605 each sulcus. We iteratively dropped the sulcus that was the dependent variable as a factor from the
606 next model to account for relationships already analyzed. Note that we excluded sulci with an
607 incidence rate of over 90% (prculs-d) and less than 15% (prculs-v, sspls-d, prcus-p, prcus-a, icgs-
608 p) due to the very small sample size.

609

610 *Marginal ramus of the cingulate sulcus types:* We quantitatively determined whether the incidence
611 rates of the four mcgs types differed by species, as well as between hemispheres for each species,
612 with $\chi 2$ tests.

613

614 Quantification of sulcal morphology

615 In the present study, we considered depth and surface area as these are two of the most defining
616 morphological features of cortical sulci — especially in PMC[15,20,24–27,29,36,38,65,71,83–89].

617

Depth: The depth of each sulcus was calculated in millimeters from each native cortical surface reconstruction. Raw values for sulcal depth were calculated from the sulcal fundus to the smoothed outer pial surface using a modified version of a recent algorithm for robust morphological statistics which builds on the Freesurfer pipeline (Madan, 2019). As the chimpanzee surfaces were scaled prior to reconstruction, we report relative (normalized) depth values for the sulci of interest. For these metrics, within each species, depth was calculated relative to the deepest point in the cortex (i.e., the insula as in previous work[15,20,38]).

Surface area: Surface area (in square millimeters) was generated for each sulcus from the *mris_anatomical_stats* function in FreeSurfer[58,90]. Again, as in prior work[38], to address scaling concerns between species, we report surface area relative to the total cortical surface area of the given hemisphere.

Morphological comparisons

To assess whether the depth and surface area of PMC sulci differed between chimpanzees and humans, for both morphological features, we ran a LME with predictors of sulcus, hemisphere, and species, as well as their interaction terms. Species, hemisphere, and sulcus were considered fixed effects. Sulcus was nested within the hemisphere which was nested within subjects. As in our prior analysis, ANOVA F-tests were applied to each model. For brevity, and considering that human PMC sulcal morphology has already been examined in prior work[20], we only report species-related effects in the main text for this set of analyses. For these analyses we did not include the *ifrms* as our prior work[20] already conducted comparative morphological analyses on this sulcus in

these two samples. Again, we excluded the sulci whose incidence rates were less than 15% in chimpanzees (prculs-v, sspls-d, prcus-p, prcus-a, icgs-p) from these analyses.

Finally, we repeated the prior analysis, exchanging the factor of PMC sulci for the mcgs branch (main branch, dorsal branch, side branch). As this is the first time these pieces have been quantitatively described, we report all effects in the main text.

Statistical analyses

All statistical tests were implemented in R (v4.0.1). LMEs were implemented with the *lme* function from *nlme* R package. ANOVA F-tests were run with the *anova* function from the built-in *stats* R package. Effect sizes for the ANOVA effects are reported with the partial eta-squared (η2) metric and computed with the *eta_squared* function from the *effectsize* R package. ANOVA chi-squared (χ2) tests were applied to each GLM, from which results were reported. GLMs were carried out with the *glm* function from the built-in *stats* R package and ANOVA χ2 tests were carried out with the *Anova* function from the *car* R package. Relevant post-hoc analyses on ANOVA effects were computed with the *emmeans* and *contrast* functions from the *emmeans* R package (*p*-values adjusted with Tukey's method). Non-ANOVA χ2 tests (for the mcgs type analysis) were carried out with the *chisq.test* function from the built-in *stats* R package. Follow-up post hoc pairwise comparisons on these χ2 tests were implemented with the *chisq.multcomp* function from the *RVAideMemoire* R package.

Data availability

Data and analysis pipelines used for this project will be made freely available on GitHub upon publication (https://github.com/cnl-berkeley/stable_projects). The colorblind-friendly color

schemes used in our figures were created using the toolbox available at https://davidmathlogic.com/colorblind/. Requests for further information should be directed to the Corresponding Author, Kevin Weiner (kweiner@berkeley.edu).

References

1. Semendeferi, K., Armstrong, E., Schleicher, A., Zilles, K. & Van Hoesen, G. W. Prefrontal cortex in humans and apes: a comparative study of area 10. *Am. J. Phys. Anthropol.* **114**, 224–241 (2001).
2. Sherwood, C. C., Broadfield, D. C., Holloway, R. L., Gannon, P. J. & Hof, P. R. Variability of Broca's area homologue in African great apes: implications for language evolution. *Anat. Rec. A Discov. Mol. Cell. Evol. Biol.* **271**, 276–285 (2003).
3. Van Essen, D. C. 4.16 - Cerebral Cortical Folding Patterns in Primates: Why They Vary and What They Signify. in *Evolution of Nervous Systems* (ed. Kaas, J. H.) 267–276 (Academic Press, 2007).
4. Parr, L. A., Hecht, E., Barks, S. K., Preuss, T. M. & Votaw, J. R. Face processing in the chimpanzee brain. *Curr. Biol.* **19**, 50–53 (2009).
5. Keller, S. S., Roberts, N. & Hopkins, W. A Comparative Magnetic Resonance Imaging Study of the Anatomy, Variability, and Asymmetry of Broca's Area in the Human and Chimpanzee Brain. *Journal of Neuroscience* vol. 29 14607–14616 Preprint at https://doi.org/10.1523/jneurosci.2892-09.2009 (2009).
6. Schenker, N. M. *et al.* Broca's area homologue in chimpanzees (Pan troglodytes): probabilistic mapping, asymmetry, and comparison to humans. *Cereb. Cortex* **20**, 730–742 (2010).

686 7. Keller, S. S., Deppe, M., Herbin, M. & Gilissen, E. Variability and asymmetry of the sulcal
687 contours defining Broca's area homologue in the chimpanzee brain. *J. Comp. Neurol.* **520**,
688 1165–1180 (2012).
689 8. Hecht, E. E. *et al.* Differences in Neural Activation for Object-Directed Grasping in
690 Chimpanzees and Humans. *J. Neurosci.* **33**, 14117–14134 (2013).
691 9. Leroy, F. *et al.* New human-specific brain landmark: the depth asymmetry of superior
692 temporal sulcus. *Proc. Natl. Acad. Sci. U. S. A.* **112**, 1208–1213 (2015).
693 10. Bruner, E., Preuss, T. M., Chen, X. & Rilling, J. K. Evidence for expansion of the
694 precuneus in human evolution. *Brain Struct. Funct.* **222**, 1053–1060 (2017).
695 11. Van Essen, D. C., Donahue, C. J. & Glasser, M. F. Development and Evolution of Cerebral
696 and Cerebellar Cortex. *Brain Behav. Evol.* **91**, 158–169 (2018).
697 12. Donahue, C. J., Glasser, M. F., Preuss, T. M., Rilling, J. K. & Van Essen, D. C. Quantitative
698 assessment of prefrontal cortex in humans relative to nonhuman primates. *Proc. Natl. Acad.*
699 *Sci. U. S. A.* **115**, E5183–E5192 (2018).
700 13. Ardesch, D. J. *et al.* Evolutionary expansion of connectivity between multimodal
701 association areas in the human brain compared with chimpanzees. *Proc. Natl. Acad. Sci. U.*
702 *S. A.* **116**, 7101–7106 (2019).
703 14. Amiez, C. *et al.* Sulcal organization in the medial frontal cortex provides insights into
704 primate brain evolution. *Nat. Commun.* **10**, 1–14 (2019).
705 15. Miller, J. A. *et al.* Sulcal morphology of ventral temporal cortex is shared between humans
706 and other hominoids. *Sci. Rep.* **10**, 17132 (2020).
707 16. Amiez, C. *et al.* Chimpanzee histology and functional brain imaging show that the
708 paracingulate sulcus is not human-specific. *Commun Biol* **4**, 54 (2021).

17. Miller, E. N., Hof, P. R., Sherwood, C. C. & Hopkins, W. D. The Paracingulate Sulcus Is a Unique Feature of the Medial Frontal Cortex Shared by Great Apes and Humans. *Brain Behav. Evol.* 1–11 (2021).

18. Sierpowska, J. *et al.* Comparing human and chimpanzee temporal lobe neuroanatomy reveals modifications to human language hubs beyond the frontotemporal arcuate fasciculus. *Proc. Natl. Acad. Sci. U. S. A.* **119**, e2118295119 (2022).

19. Hopkins, W. D. *et al.* A comprehensive analysis of variability in the sulci that define the inferior frontal gyrus in the chimpanzee (*Pan troglodytes*) brain. *American Journal of Biological Anthropology* **179**, 31–47 (2022).

20. Willbrand, E. H. *et al.* Uncovering a tripartite landmark in posterior cingulate cortex. *Science Advances* **8**, eabn9516 (2022).

21. Zilles, K., Palomero-Gallagher, N. & Amunts, K. Development of cortical folding during evolution and ontogeny. *Trends Neurosci.* **36**, 275–284 (2013).

22. Zilles, K., Armstrong, E., Schleicher, A. & Kretschmann, H.-J. The human pattern of gyrification in the cerebral cortex. *Anatomy and Embryology* vol. 179 173–179 Preprint at https://doi.org/10.1007/bf00304699 (1988).

23. Amiez, C., Wilson, C. R. E. & Procyk, E. Variations of cingulate sulcal organization and link with cognitive performance. *Sci. Rep.* **8**, 1–13 (2018).

24. Weiner, K. S. The Mid-Fusiform Sulcus (sulcus sagittalis gyri fusiformis). *Anat. Rec.* **302**, 1491–1503 (2019).

25. Willbrand, E. H., Ferrer, E., Bunge, S. A. & Weiner, K. S. Development of human lateral prefrontal sulcal morphology and its relation to reasoning performance. *bioRxiv* 2022.09.14.507822 (2022) doi:10.1101/2022.09.14.507822.

26. Willbrand, E. H., Voorhies, W. I., Yao, J. K., Weiner, K. S. & Bunge, S. A. Presence or absence of a prefrontal sulcus is linked to reasoning performance during child development. *Brain Struct. Funct.* **227**, 2543–2551 (2022).

27. Voorhies, W. I., Miller, J. A., Yao, J. K., Bunge, S. A. & Weiner, K. S. Cognitive insights from tertiary sulci in prefrontal cortex. *Nat. Commun.* **12**, 5122 (2021).

28. Yao, J. K., Voorhies, W. I., Miller, J. A., Bunge, S. A. & Weiner, K. S. Sulcal depth in prefrontal cortex: a novel predictor of working memory performance. *Cereb. Cortex* bhac173 (2022).

29. Lopez-Persem, A., Verhagen, L., Amiez, C., Petrides, M. & Sallet, J. The Human Ventromedial Prefrontal Cortex: Sulcal Morphology and Its Influence on Functional Organization. *J. Neurosci.* **39**, 3627–3639 (2019).

30. Fornito, A. *et al.* Individual differences in anterior cingulate/paracingulate morphology are related to executive functions in healthy males. *Cereb. Cortex* **14**, 424–431 (2004).

31. Fornito, A. *et al.* Morphology of the paracingulate sulcus and executive cognition in schizophrenia. *Schizophr. Res.* **88**, 192–197 (2006).

32. Cachia, A. *et al.* The shape of the ACC contributes to cognitive control efficiency in preschoolers. *J. Cogn. Neurosci.* **26**, 96–106 (2014).

33. Garrison, J. R. *et al.* Paracingulate sulcus morphology is associated with hallucinations in the human brain. *Nat. Commun.* **6**, 8956 (2015).

34. Miller, J. A., D'Esposito, M. & Weiner, K. S. Using Tertiary Sulci to Map the 'Cognitive Globe' of Prefrontal Cortex. *J. Cogn. Neurosci.* 1–18 (2021).

35. Hopkins, W. D. *et al.* Sulcal Morphology in Cingulate Cortex is Associated with Voluntary Oro-Facial Motor Control and Gestural Communication in Chimpanzees (Pan troglodytes).

Cereb. Cortex **31**, 2845–2854 (2021).

36. Miller, J. A., Voorhies, W. I., Lurie, D. J., D'Esposito, M. & Weiner, K. S. Overlooked Tertiary Sulci Serve as a Meso-Scale Link between Microstructural and Functional Properties of Human Lateral Prefrontal Cortex. *J. Neurosci.* **41**, 2229–2244 (2021).

37. Parker, B. J. *et al.* Hominoid-specific sulcal variability is related to face perception ability. *bioRxiv* 2022.02.28.482330 (2022) doi:10.1101/2022.02.28.482330.

38. Hathaway, C. B. *et al.* Defining tertiary sulci in lateral prefrontal cortex in chimpanzees using human predictions. *bioRxiv* 2022.04.12.488091 (2022) doi:10.1101/2022.04.12.488091.

39. Parvizi, J., Van Hoesen, G. W., Buckwalter, J. & Damasio, A. Neural connections of the posteromedial cortex in the macaque. *Proc. Natl. Acad. Sci. U. S. A.* **103**, 1563–1568 (2006).

40. ten Donkelaar, H. J. T., ten Donkelaar, H. J., Tzourio-Mazoyer, N. & Mai, J. K. Toward a Common Terminology for the Gyri and Sulci of the Human Cerebral Cortex. *Frontiers in Neuroanatomy* vol. 12 Preprint at https://doi.org/10.3389/fnana.2018.00093 (2018).

41. ten Donkelaar, H. J., Kachlík, D. & Shane Tubbs, R. *An Illustrated Terminologia Neuroanatomica: A Concise Encyclopedia of Human Neuroanatomy*. (Springer, 2018).

42. Raichle, M. E. *et al.* A default mode of brain function. *Proc. Natl. Acad. Sci. U. S. A.* **98**, 676–682 (2001).

43. Buckner, R. L., Andrews-Hanna, J. R. & Schacter, D. L. The brain's default network: anatomy, function, and relevance to disease. *Ann. N. Y. Acad. Sci.* **1124**, 1–38 (2008).

44. Margulies, D. S. *et al.* Precuneus shares intrinsic functional architecture in humans and monkeys. *Proc. Natl. Acad. Sci. U. S. A.* **106**, 20069–20074 (2009).

778 45. Kong, R. *et al.* Spatial Topography of Individual-Specific Cortical Networks Predicts
779 Human Cognition, Personality, and Emotion. *Cereb. Cortex* **29**, 2533–2551 (2019).
780 46. Smallwood, J. *et al.* The default mode network in cognition: a topographical perspective.
781 *Nat. Rev. Neurosci.* **22**, 503–513 (2021).
782 47. Foster, B. L. *et al.* A tripartite view of the posterior cingulate cortex. *Nat. Rev. Neurosci.*
783 (2022) doi:10.1038/s41583-022-00661-x.
784 48. Hagmann, P. *et al.* Mapping the Structural Core of Human Cerebral Cortex. *PLoS Biology*
785 vol. 6 e159 Preprint at https://doi.org/10.1371/journal.pbio.0060159 (2008).
786 49. Grydeland, H., Westlye, L. T., Walhovd, K. B. & Fjell, A. M. Intracortical Posterior
787 Cingulate Myelin Content Relates to Error Processing: Results from T1- and T2-Weighted
788 MRI Myelin Mapping and Electrophysiology in Healthy Adults. *Cereb. Cortex* **26**, 2402–
789 2410 (2016).
790 50. Leech, R. & Sharp, D. J. The role of the posterior cingulate cortex in cognition and disease.
791 *Brain* **137**, 12–32 (2014).
792 51. Pearson, J. M., Heilbronner, S. R., Barack, D. L., Hayden, B. Y. & Platt, M. L. Posterior
793 cingulate cortex: adapting behavior to a changing world. *Trends in Cognitive Sciences* vol.
794 15 143–151 Preprint at https://doi.org/10.1016/j.tics.2011.02.002 (2011).
795 52. Schacter, D. L., Addis, D. R. & Buckner, R. L. Remembering the past to imagine the future:
796 the prospective brain. *Nature Reviews Neuroscience* vol. 8 657–661 Preprint at
797 https://doi.org/10.1038/nrn2213 (2007).
798 53. Miller, J. A. & Weiner, K. S. Unfolding the evolution of human cognition. *Trends Cogn.*
799 *Sci.* **26**, 735–737 (2022).
800 54. de Abreu, T. *et al.* Comparative anatomy of the encephalon of new world primates with

emphasis for the Sapajus sp. *PLoS One* **16**, e0256309 (2021).

55. Bailey, P., Bonin, G. V. & McCulloch, W. S. The isocortex of the chimpanzee. Vol. 440 University of Illinois Press. *Urbana* (1950).

56. Retzius, Gustaf. *Cerebra simiarum illustrata. Das Affenhirn in bildlicher Darstellung*. 304 (Stockholm,Centraldruckerei;, 1906).

57. Destrieux, C., Fischl, B., Dale, A. & Halgren, E. Automatic parcellation of human cortical gyri and sulci using standard anatomical nomenclature. *Neuroimage* **53**, 1–15 (2010).

58. Dale, A. M., Fischl, B. & Sereno, M. I. Cortical surface-based analysis. I. Segmentation and surface reconstruction. *Neuroimage* **9**, 179–194 (1999).

59. Vogt, B. A., Nimchinsky, E. A., Vogt, L. J. & Hof, P. R. Human cingulate cortex: surface features, flat maps, and cytoarchitecture. *J. Comp. Neurol.* **359**, 490–506 (1995).

60. Petrides, M. *Atlas of the Morphology of the Human Cerebral Cortex on the Average MNI Brain*. (Academic Press, 2019).

61. Ono, M., Kubik, S. & Abernathey, C. D. *Atlas of the Cerebral Sulci*. (G. Thieme Verlag, 1990).

62. Campbell, A. W. *Histological studies on the localisation of cerebral function*. (Cambridge University Press, 1905).

63. Bailey, P. & von Bonin, G. *The Isocortex of Man*. (University of Illinois Press, 1951).

64. Chiavaras, M. M. & Petrides, M. Orbitofrontal sulci of the human and macaque monkey brain. *J. Comp. Neurol.* **422**, 35–54 (2000).

65. Weiner, K. S. *et al.* The mid-fusiform sulcus: a landmark identifying both cytoarchitectonic and functional divisions of human ventral temporal cortex. *Neuroimage* **84**, 453–465 (2014).

66. Drudik, K., Zlatkina, V. & Petrides, M. Morphological patterns and spatial probability maps of the superior parietal sulcus in the human brain. *Cereb. Cortex* (2022) doi:10.1093/cercor/bhac132.

67. Cavanna, A. E. & Trimble, M. R. The precuneus: a review of its functional anatomy and behavioural correlates. *Brain* **129**, 564–583 (2006).

68. Hill, J. *et al.* Similar patterns of cortical expansion during human development and evolution. *Proc. Natl. Acad. Sci. U. S. A.* **107**, 13135–13140 (2010).

69. Connolly, C. J. Development of the cerebral sulci. *Am. J. Phys. Anthropol.* **26**, 113–149 (1940).

70. Connolly, C. J. *External morphology of the primate brain*. (CC Thomas, 1950).

71. Armstrong, E., Schleicher, A., Omran, H., Curtis, M. & Zilles, K. The ontogeny of human gyrification. *Cereb. Cortex* **5**, 56–63 (1995).

72. Cunningham, D. J. *Contribution to the Surface Anatomy of the Cerebral Hemispheres*. (Academy House, 1892).

73. Malikovic, A. *et al.* Occipital sulci of the human brain: variability and morphometry. *Anat. Sci. Int.* **87**, 61–70 (2012).

74. Gurer, B. *et al.* An Anatomical Study. *Clin. Anat.* **26**, 667–674 (2013).

75. Dziedzic, T. A., Bala, A. & Marchel, A. Cortical and Subcortical Anatomy of the Parietal Lobe From the Neurosurgical Perspective. *Front. Neurol.* **12**, 727055 (2021).

76. Chapman, H. C. On the Structure of the Chimpanzee. *Proceedings of the Academy of Natural Sciences of Philadelphia* **31**, 52–63 (1879).

77. Walker, A. E. & Fulton, J. F. The External Configuration of the Cerebral Hemispheres of the Chimpanzee. *J. Anat.* **71**, 105–116.9 (1936).

847 78. Hopkins, W. D. *et al.* Genetic Factors and Orofacial Motor Learning Selectively Influence
848 Variability in Central Sulcus Morphology in Chimpanzees (Pan troglodytes). *J. Neurosci.*
849 **37**, 5475–5483 (2017).
850 79. Becker, Y. *et al.* Broca's cerebral asymmetry reflects gestural communication's
851 lateralisation in monkeys (Papio anubis). *Elife* **11**, (2022).
852 80. Glasser, M. F. *et al.* The minimal preprocessing pipelines for the Human Connectome
853 Project. *Neuroimage* **80**, 105–124 (2013).
854 81. Hopkins, W. D., Li, X., Crow, T. & Roberts, N. Vertex- and atlas-based comparisons in
855 measures of cortical thickness, gyrification and white matter volume between humans and
856 chimpanzees. *Brain Struct. Funct.* **222**, 229–245 (2017).
857 82. Borne, L., Rivière, D., Mancip, M. & Mangin, J.-F. Automatic labeling of cortical sulci
858 using patch- or CNN-based segmentation techniques combined with bottom-up geometric
859 constraints. *Med. Image Anal.* **62**, 101651 (2020).
860 83. Sanides, F. Structure and function of the human frontal lobe. *Neuropsychologia* **2**, 209–219
861 (1964).
862 84. Chi, J. G., Dooling, E. C. & Gilles, F. H. Gyral development of the human brain. *Ann.*
863 *Neurol.* **1**, 86–93 (1977).
864 85. Welker, W. Why Does Cerebral Cortex Fissure and Fold? in *Cerebral Cortex: Comparative*
865 *Structure and Evolution of Cerebral Cortex, Part II* (eds. Jones, E. G. & Peters, A.) 3–136
866 (Springer US, 1990).
867 86. Weiner, K. S., Natu, V. S. & Grill-Spector, K. On object selectivity and the anatomy of the
868 human fusiform gyrus. *Neuroimage* **173**, 604–609 (2018).
869 87. Alemán-Gómez, Y. *et al.* The human cerebral cortex flattens during adolescence. *J.*

Neurosci. **33**, 15004–15010 (2013).

88. Madan, C. R. Robust estimation of sulcal morphology. *Brain Inform* **6**, 5 (2019).

89. Natu, V. S. *et al.* Sulcal Depth in the Medial Ventral Temporal Cortex Predicts the Location of a Place-Selective Region in Macaques, Children, and Adults. *Cereb. Cortex* **31**, 48–61 (2021).

90. Fischl, B., Sereno, M. I. & Dale, A. M. Cortical surface-based analysis. II: Inflation, flattening, and a surface-based coordinate system. *Neuroimage* **9**, 195–207 (1999).